Classification and lift-off height prediction of non-premixed MILD and autoignitive flames

M.J. Evans [a, b, *], P.R. Medwell [a], H. Wu [b], A. Stagni [b, c], M. Ihme [b]

[a] *School of Mechanical Engineering, The University of Adelaide, South Australia 5005, Australia*
[b] *Department of Mechanical Engineering, Stanford University, California 94305, USA*
[c] *Dipartimento di Chimica, Materiali ed Ingegneria Chimica "G. Natta", Politecnico di Milano, 20133 Milan, Italy*

Received 4 December 2015; accepted 1 June 2016

Abstract

Moderate or intense low oxygen dilution (MILD) combustion has been the subject of numerous studies in recent years. An issue remains, however, in the definition of the boundaries of the MILD combustion regime with respect to non-premixed configurations without predefined reference temperatures. A flamelet definition is applied to non-premixed configurations to better understand the MILD combustion regime and classify previous experimental investigations. Through a simplified analysis, a new definition for the non-premixed MILD combustion regime is derived. This new definition is a function of initial and final temperatures, and the effective activation energy of an equivalent one-step chemical reaction. This inherently agrees with the features of the premixed flamelet definition and provides insight into previous attempts to reconcile premixed and non-premixed classifications of MILD combustion. Previously studied turbulent flames are classified using the new definition of MILD combustion and are compared to experimental observations. The new definition of MILD combustion is subsequently compared to the ignition characteristics of opposed-flow ethylene flames, showing good agreement. Finally, transient flamelets are solved for a modelled flow-field to successfully reproduce non-monotonic trends in the lift-off that is observed experimentally in a series of MILD and autoignitive, turbulent ethylene flames in hot, diluted coflows.

Keywords: MILD combustion; Non-premixed flames; Lifted flames; Autoignition; Flamelet theory

1. Introduction

Moderate or intense low oxygen dilution (MILD) combustion features reduced pollutant emissions and efficiency improvements over conventional combustion [1]. Operation in the MILD, or flameless, combustion regime is generally achieved by burning fuel in hot, low oxygen environments. This reduces chemical reaction rates,

* Corresponding author at: School of Mechanical Engineering, The University of Adelaide, South Australia, 5005, Australia. Fax: +61 8 8313 4367.
E-mail address: m.evans@adelaide.edu.au (M.J. Evans).

Nomenclature

α	Heat release parameter
χ	Scalar dissipation rate
ΔT	Temperature increase
ω	Reaction rate
ρ	Density
τ	Non-dimensional time
θ	Non-dimensional temperature
D	Jet exit diameter
Da	Global Damköhler number
E_{eff}	Effective one-step activation energy
R	Universal gas constant
r	Radius (cylindrical polar coordinates)
Sc_t	Turbulent Schmidt number
T	Temperature
u_0	Jet bulk velocity relative to coflow velocity
x	Axial distance from jet exit plane

Subscripts

0	Reference value
b	Fully burnt mixture
$cofl$	Coflow conditions
ex	Extinction condition
ign	Steady-state autoignition condition
in	Initial condition
mr	Most reactive mixture
si	Self-ignition condition
st	Stoichiometric mixture
u	Unburnt (fresh) mixture

resulting in distributed reaction zones as opposed to the high temperature peaks in conventional flames [1]. As a result, jet flames in the MILD regime feature a global Damköhler number (Da) near unity, such that finite-rate chemistry becomes important [2,3]. Despite numerous investigations into the unique characteristics of MILD combustion, the boundaries of the MILD regime have not been thoroughly defined in non-premixed configurations.

Ignition and combustion stability of the MILD combustion regime have been investigated experimentally [4] and numerically [4–7] in premixed reactors [1]. These analyses have been based on initial temperature (T_{in}) and temperature increase (ΔT), relative to a self-ignition temperature (T_{si}) [1]. This T_{si} is defined as the minimum inlet temperature required for ignition in a perfectly-stirred reactor (PSR) within one second [1]. This definition has since formed the basis of premixed [4–6] and non-premixed [8] analyses of MILD combustion.

The MILD combustion regime in a premixed reactor has been defined independently to T_{si} [1,5]. By this definition, MILD combustion implies that the S-shaped curve of temperature as a function of the characteristic time is monotonic, and without ignition or extinction points [5,9–11]. This definition leads to a criterion for premixed MILD combustion, which, assuming constant specific heat at constant pressure, may be approximated as [1]:

$$E_{eff}/(RT_{in}) \leq 4(1 + T_{in}/\Delta T) \quad (1)$$

where R is the universal gas constant and E_{eff} is the effective activation energy of an equivalent one-step reaction. This definition separates gradually igniting MILD flames from conventional autoignitive flames, which feature ignition and extinction points on the S-shaped curve. This is consistent with the "flameless" description of MILD combustion [1,5]. The two alternate premixed classifications of MILD combustion both propose distinct definitions of the MILD regime, based on a critical temperature, T_{si}, [1] or the global ignition process, E_{eff} [5].

The definition of MILD combustion based on the S-shaped curve has previously been applied in analytical [9] and numerical [10,11] studies. A previous analytical study combined the monotonic S-shaped curve with a pre-defined quenching temperature, to enforce an extinction condition [9]. The S-shaped curve concept has additionally been used to classify results in a numerical study, with extinction disappearing with sufficient preheating and dilution [11].

Experimental studies of non-premixed ethylene (C_2H_4) flames in a jet-in-hot-coflow (JHC) burner indicate that apparently attached flames undergo gradual ignition in low oxygen coflows, corresponding to MILD combustion [12,13]. Increasing oxygen concentration leads to a transition to a conventional autoignitive flame structure [12–14]. Both flame structures were observed by Medwell et al. [12] in two flames meeting the PSR definition of MILD combustion, despite their different ignition characteristics.

The numerical investigation of MILD combustion in a JHC configuration added "quasi-MILD" and "MILD-like" regimes [8] to the PSR definition of Cavaliere and de Joannon [1]. Both regimes keep the condition $\Delta T < T_{si}$, however, the former describes cases requiring forced ignition and the latter does not meet the imposed "low oxygen dilution" criterion [8]. Neither [8], nor the subsequent chemical kinetics analysis [6] offer further distinctions between MILD combustion and these two regimes. These classifications expand the PSR definition, however are unable to distinguish gradual MILD combustion from conventional autoignition.

The definitions of MILD combustion based on temperatures are not consistent between premixed and non-premixed configurations. The current work aims to use an idealised, one-dimensional flamelet analysis to define non-premixed MILD combustion without the requirement for composition-dependent reference temperatures, by including a fuel-specific E_{eff}. This definition is based on the S-shaped curve

concept [5,9] which is applied to non-premixed configurations through analysis similar to that by Pitsch and Fedotov [15]. This new definition for non-premixed MILD combustion is quantified through an opposed-flow flamelet analysis, to produce a criterion for non-premixed MILD combustion, which is compared to premixed regime classifications. This definition is subsequently used to classify previous experiments, and compare flamelet simulations to new experimental observations in a JHC burner.

2. Numerical analysis

2.1. Non-premixed flamelet analysis

The one-dimensional, opposed-flow flamelet equations for a non-premixed system with an irreversible, one-step reaction were analysed by Pitsch and Fedotov [15]. This analysis couples the reaction rate (ω), scalar dissipation rate (χ), mixture fraction (Z) and normalised time (τ). At stoichiometric conditions (st), the flamelet solution was shown to yield the following equation relating normalised temperature (θ_{st}) and χ along the S-shaped curve [15]:

$$\frac{d\theta_{st}}{d\tau} + (\chi_{st}/\chi_{st,0})\theta_{st} - \omega(\theta_{st}) = 0 \tag{2}$$

with $\theta = (T - T_{st,u})/\Delta T$ and:

$$\omega = Da(1-\theta_{st})^2 \frac{(1-\alpha)\exp(\beta_0 - \beta)}{1-\alpha(1-\theta_{st})} \times \exp\left(-\alpha\beta\frac{1-\theta_{st}}{1-\alpha(1-\theta_{st})}\right) \tag{3}$$

where $\alpha = \Delta T_{st}/T_{st,b}$ is the heat release parameter, $\beta = E_{eff}/(RT_{st,b})$ is the activation temperature ratio, u refers to the unburnt (fresh) mixture, b indicates fully-burnt, 0 indicates a reference value and Da is constant for any given fuel and oxidant combination. Differentiation of Eq. (3) with respect to θ_{st}, at steady-state, produces the condition for turning points in the S-shaped curve ($\frac{\partial \chi_{st}}{\partial \theta_{st}} = 0$), on the interval $0 < \theta_{st} < 1$:

$$\zeta = (\beta^2 + 6\beta + 1)\alpha^2 - (6\beta - 2)\alpha + 1 \geq 0 \tag{4}$$

Satisfying this condition implies turning points exist in the curve χ_{st} versus θ_{st}, corresponding to ignition (ig) and extinction (ex) given by:

$$\theta_{st} = 1 - \frac{1 + (3+\beta)\alpha \pm \zeta^{1/2}}{2(\alpha^2 + (1+\beta)\alpha)}, \quad \theta_{st,ex} \geq \theta_{st,ign} \tag{5}$$

If $\theta_{st,\,ign}$ and $\theta_{st,\,ex}$ are real, the S-shaped curve features autoignition and extinction. If these are complex, $\zeta < 0$, then χ_{st} versus θ_{st} is monotonic, indicating MILD combustion [5]. Finally, negative values indicate no physical solution.

2.2. S-Shaped curve generation

Sixty-three S-shaped curves with C_2H_4 fuel were simulated in FlameMaster [16]. The FlameMaster code uses a finite difference method solved on an adaptive mesh with a second-order, implicit backward difference formula. These S-shaped curve solutions were used to form a map of $\theta_{st,ex} - \theta_{st,ign}$ (see Eq. (5)), with MILD combustion identified if $\theta_{st,ex} - \theta_{st,ign}$ was zero or could not be evaluated. Oxidisers ranged from 1000 K to 1600 K, at intervals of 100 K, and composed of 2–15% O_2 by volume, at increments of 1% from 2–9% and then every 2% to 15%. The oxidisers consisted of 10% H_2O and 3% CO_2, balanced by N_2 [12]. These were solved using the C1–C3 sub-mechanism from the December 2014 version of the detailed POLIMI mechanism for hydrocarbon combustion [17].

2.3. Transient flamelet analysis

The ignition of MILD and conventional autoignitive flames was analysed using two-dimensional profiles for Z and χ. This procedure is similar to previous analyses of turbulent jet flames using transient, opposed-flow flamelets [18]. A conical potential core was imposed for the mixture fraction with a length of 7 x/D. Further downstream ($x/D \geq 7$), the Z profile was taken from the self-similar analysis by [19]:

$$x/D < 7: \quad Z = \begin{cases} 1, & R(x) < 0 \\ \left(1 + [\gamma R_\eta(x)]^2/4\right)^{-2Sc_t}, & R(x) \geq 0 \end{cases}$$
$$x/D \geq 7: \quad Z = \frac{70}{32}\frac{(1+2Sc_t)D}{(x+x_0)(\rho_0\rho_{st})^{1/2}}\left(1 + \frac{[\gamma\eta]^2}{4}\right)^{-2Sc_t} \tag{6}$$

where $\gamma = [3 \times 70^2/(64\rho_{st})]^{1/2}$ [19]; $\eta = r_\rho D/(x + x_0)$ [19]; $x_0 = [70/32(1+2Sc_t)\rho_{st} - 7]D$; $R(x) = [1 - x/(7D)]/2$ and:

$$R_\eta(x) = \frac{[r_\rho - R(x)]D}{x + [1 - x/(7D)]x_0} \tag{7}$$

$$r_\rho = D^{-1}\left(2\int_0^r \frac{\rho}{\rho_{cofl}} r' dr'\right)^{1/2} \tag{8}$$

with $Sc_t = 0.71$ [19]. Values of $D = 4.6$ mm, $\rho_0 = 1.26$ kg/m^3, $\rho_{cofl} = 0.31$ kg/m^3 and $\rho_{st} = 0.20$ kg/m^3 and $u_0 = 15.2$ m/s were taken from experimental conditions. Density was taken to be the linear mixture of the fuel and oxidant streams. Finally, the profile of χ was taken as [18,20]:

$$\chi = u_0/(35Sc_t D)(\rho_0/\rho)^2\left|\frac{dZ}{dr_\rho}\right|^2 \tag{9}$$

Fuel and oxidiser streams were matched to the current experimental C_2H_4 flames in 1250-K coflows of 3%, 6% and 9% O_2 by volume with $Z_{st} = 0.01$,

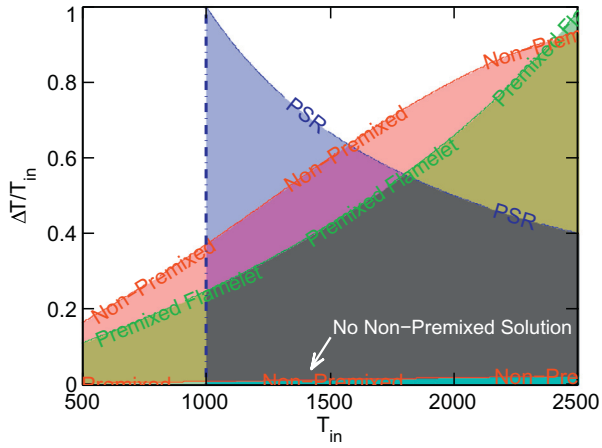

Fig. 1. Combined regime map for MILD combustion according to three different definitions: PSR [1] (blue), premixed flamelet [5] (green), and non-premixed flamelet (red). With $T_{si} = 1000$ K, $E_{eff} = 1.67 \times 10^8$ J/kmol [1] and $T_{in} = T_{st,u}$.(For interpretation of the references to colour in this figure legend, the reader is referred to the web version of this article).

0.02 and 0.03, respectively. Flames with hot oxidisers initially ignite at the most-reactive mixture fraction (Z_{mr}) $< Z_{st}$, with the maximum reaction rate [21]. Although Z_{mr} is not strongly dependent on χ, higher χ increase ignition delays [21]. Changes in the reactant streams may shift Z_{mr} and the ignition location, resulting in significantly different ignition delays. The flamelets were solved using the USC-II C1-C4 chemical kinetics mechanism [22]. A stoichiometric flamelet velocity described the downstream motion of Z_{st} in time [18], based on a self-similar jet velocity profile [19]. Higher values of Z_{st} are closer to the faster fuel jet, and hence have higher flamelet velocities. The stoichiometric flamelet velocity was subsequently used to remap times to corresponding x/D for analysis.

3. Experimental details

Chemiluminescence images were taken of C_2H_4 flames in a previously studied JHC burner [12]. Chemiluminescence of OH^* is spontaneous UV emission from excited OH. The peak intensity of OH^* concentration has been shown to correspond to peak flame temperatures in laminar flames [11]. Imaging of OH^* chemiluminescence may be therefore used to qualitatively identify the highest temperature regions of a flame.

Fuel issues from a 4.6-mm diameter central jet at a Reynolds number near 10,000 into 2.8 m/s coflows with measured coflow temperatures (T_{coft}) of 1250 K and 3–11% O_2. These coflows also include 10.7% H_2O and 3.6% CO_2 by volume, balanced with N_2. These compositions are similar to previous experiments [12], which are used for the C_2H_4 regime map. This configuration provides a controlled environment for approximately 100 mm downstream of the coflow exit plane. Flames are imaged using a pco.pixelfly camera with a Lambert Instruments intensifier. An f-number 3.5, UV transmissive lens is fitted with a 310 nm optical filter with a bandwidth of 10 nm. Mean images are formed from a series of 50 images, each taken with a gate time of 1 ms and corrected for background.

4. Results and discussion

4.1. MILD combustion definitions

Different definitions of MILD combustion are shown overlaid in Fig. 1. The values of $T_{si} = 1000$ K and $E_{eff} = 1.67 \times 10^8$ J/kmol (40 kcal/mol) are chosen from reference [1]. The blue region indicates the PSR definition of Cavaliere and de Joannon [1], bounded by $\Delta T \leq T_{si}$; the premixed S-shaped curve definition of Oberlack et al. [5], where Eq. (1) holds, is in green; and the current non-premixed study, where the condition in Eq. (4) is not met, is shown in red. The overlap between the domains indicates that both gradual ignition and conventional autoignition flame structures exist within the boundaries of the PSR defined regime. This indicates that the PSR regime includes flames featuring instabilities due to local autoignition and extinction, and those which are devoid of local extinction or sharp peaks in flame temperature, which are consistent with the physical description of MILD combustion [1]. This is consistent with previous experimental investigations of ethylene 3% O_2 and 9% O_2 oxidants which exhibit significant differences in structure [12], despite both conditions meeting the PSR definition of MILD combustion [1]. The PSR definition simply limits the maximum flame temperature to $T_{in} + T_{si}$, whereas

the definitions based on the S-shaped curves indicate the shift from gradual ignition to autoignition. The maximum flame temperature of the S-shaped curve-based MILD regimes, however, increase with T_{in}, highlighting inconsistency between $\Delta T = T_{st,b} - T_{st,u} \leq T_{si}$ and the flame ignition characteristics. This supports the use of the new MILD combustion definition for predicting ignition behaviour of non-premixed flames.

Combustion is apparent well below the predefined $T_{in} = 1000$ K PSR threshold [1] shown in Fig. 1. This region exhibits what Wang et al. [6,8] term "quasi-MILD" combustion, which requires an external ignition source. This indicates MILD combustion occurring under forced ignition [6,8], in contrast to the $T_{in} \geq T_{si}$ requirement of the PSR definition [1]. In this sense, the new MILD definition predicts "quasi-MILD" behaviour suggested by Wang et al. [6,8]. The region of "MILD-like" combustion [6,8] cannot, however, be determined from this generalised figure which makes no reference to oxygen levels.

Of the flamelet regimes in Fig. 1, the non-premixed MILD regime allows for greater ΔT compared to the premixed case for most T_{in}. At higher T_{in}, however, the non-premixed limit begins to approach a limiting value whilst the maximum $\Delta T/T_{in}$ for the premixed MILD regime continues to increase. Additionally, the analysis features a region of low $\Delta T/T_{in}$ where a non-premixed solution does not exist. These effects demonstrate the differences between premixed and non-premixed flames, despite qualitatively similar trends and descriptions of MILD combustion. These different trends show that for a given fuel of some E_{eff}, there is a limiting value of $\Delta T/T_{in}$ for non-premixed MILD flames which does not exist in premixed configurations.

4.2. *Non-premixed regime maps*

The MILD regime map in Fig. 1 may be expanded to arbitrary fuel and oxidant combinations on the α and β axes. The regime diagram in Fig. 2 shows shaded contours of $\theta_{st,\,ign}$, defined by Eq. (5), in the three distinct regions for different fuels with specific E_{eff}.

A selection of experimental cases are included in Fig. 2 to classify flames as either MILD or autoignitive flames. E_{eff} is taken to be 2.51×10^8 J/kmol (60 kcal/mol) [23] for all cases using CH_4-based fuels. These are HM1-3 cases using a CH_4-H_2 blend [24], the Delft JHC (DJHC) using Dutch natural gas [25], the F1, F4 and F7 cases using pure CH_4 [26] and CH_4-air flame of Cabra et al. [27]. One set of data for pure C_2H_4 fuels is included [12] with $E_{eff} = 1.26 \times 10^8$ J/kmol (30 kcal/mol) [28]. The classification of the HM1-3 flames agrees with previously simulated S-shaped curves, which indicate autoignition in the two cases with the greatest %O_2 coflows [10]. The cases for oxidants with 3% O_2 in the studies from Medwell et al. [12] and Dally et al. [24] are within the MILD regime, whereas the remaining flames with oxidant $O_2 \sim 7$–10%, are autoignitive. This is consistent with the experimentally observed structures of these flames [12,24–27]. This is in spite of some of these flames [12,25] meeting the PSR conditions of MILD combustion [1].

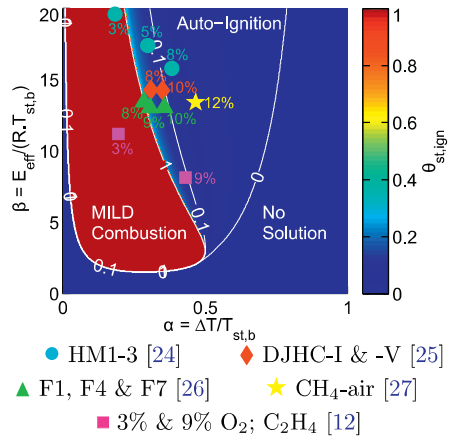

Fig. 2. Normalised autoignition temperature, $\theta_{st,\,ign}$, for a range of α and β and showing experimental cases with coflow O_2 concentrations as percentage of volume.

The regime diagram in Fig. 2 separates MILD and autoignitive flames and may be used to predict the structure of flames from evaluation of the initial mixing temperature $T_{st,\,u}$, adiabatic flame temperature $T_{st,\,b}$ and E_{eff} for a given fuel. This regime map shows the limited achievable range of α with almost constant β using CH_4/air coflows [25,26]. Both the HM1-3 and C_2H_4 sets of flames, ignite at almost constant $T_{st,\,u}$ with varying concentrations of O_2. This highlights the necessity of studying ignition in coflows with different fuels and diluents which can access a wider range of operating conditions [12,24].

The regime diagram in Fig. 2 shows a region of significant temperature increase followed by autoignition ($\theta_{st,\,ign} > 10\%$), which may be indicative of the "transitional" flames described by Medwell et al. [12]. The width of this region increases with β, implying precursor reactions with significant heat release are more prominent for high β, or low $T_{st,\,b}$. Additionally, increasing $T_{st,\,u}$ with constant ΔT results in lower β. This shows that MILD combustion is most readily achievable for high $T_{st,\,u}$, however may be achieved at any $T_{st,\,u}$ with sufficiently low ΔT, consistent with the premixed definition [5] and the regimes of Wang et al. [6,8].

Figure 3 presents regimes of stoichiometric ethylene combustion as a function of oxidant O_2 molar concentration and initial mixture temperature. This figure shows a pair of previously studied flames [12], and flame conditions to be

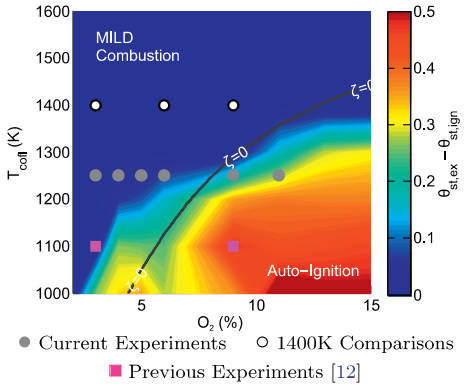

Fig. 3. Contours of $\theta_{st,ex} - \theta_{st,ign}$ for C_2H_4 flamelets on T_{coft} and O_2 axes, with the boundary between MILD and autoignition regimes ($\zeta = 0$) from Eq. (4).

examined in the next section. The line of $\zeta = 0$ (see Eq. (4)) with $E_{eff} = 1.26 \times 10^8$ J/kmol [28] is plotted over these contours, and shows very good agreement in the location of the MILD combustion regime boundary. Discrepancies in the lower-left corner of the figure are due to small $\theta_{st,ex} - \theta_{st,ign} < 100$ K. These ignition events are the result of two-stage ignition processes not captured by the cubic S-shaped curve of the analytical model. In these flames, autoignition occurs after significant, gradual increases in temperature, which are reminiscent of gradual MILD ignition. Additionally, this may be indicative of non-unity Lewis number effects in the flamelet analyses, neglected in deriving ζ.

The good agreement between regime boundaries in Fig. 3 implies that both autoignition and MILD combustion may be analysed with single-step reactions. In such analyses, different conditions and chemical pathways could be accounted for with rate coefficients which are functions of the fuel and oxidant compositions, and the local mixture fraction. This is in contrast to previous modelling of similar flames which stressed the importance of multi-step kinetics [2]. These results suggest the potential effectiveness of one-step reaction models, using functions as rate coefficients, near the limits of autoignition.

4.3. *Chemiluminescence of jet flames*

Chemiluminescence of excited hydroxyl from a series of turbulent C_2H_4 jet flames issuing into hot and diluted coflows are shown in Fig. 4. The regime diagram in Fig. 3 indicates that the flames issuing into the 9% and 11% O_2 coflows should be autoignitive, with the remainder in the MILD regime. These images show strong OH* emissions near the base of the autoignitive flames which are not apparent in the MILD flames. The OH* signal may be used as a qualitative indicator of regions of peak temperatures [11]. Well-defined lift-off heights of 8 mm and

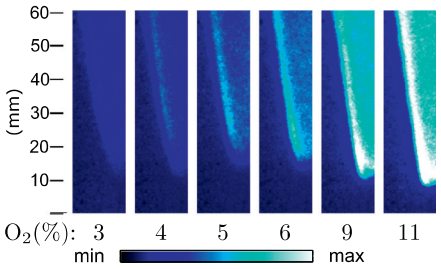

Fig. 4. Images of OH* emissions from turbulent C_2H_4 flames in 1250-K coflows with different %O_2 (by vol.) averaged over 50 × 1 ms images. The height is given in millimetres, with the lower edge of the images at the jet exit plane. Images are 16 mm × 60 mm and corrected for background.

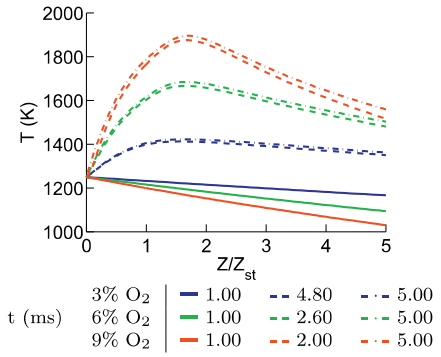

Fig. 5. T vs. Z/Z_{st} profiles of transient flamelets at different times for C_2H_4 fuel in 1250-K coflows.

11 mm ($x/D = 1.7$ and 2.4) are seen for the flames in 11% and 9% O_2 coflows, with less distinct lift-off heights of approximately 14 mm ($x/D = 3.0$) in 5% and 6% O_2 coflows. No OH* chemiluminescence is detectable below these points for any camera and intensifier exposure times. Chemiluminescent emissions are discernible in the 3% and 4% O_2 cases from 11 mm downstream of the jet exit, following adjustments of the colour-scale (not shown for brevity). Below these locations, any OH* emission is below the measurement threshold of the equipment. This trend in lift-off heights demonstrate gradual ignition in MILD combustion in low O_2 coflows, and the transition to conventional autoignition with increasing O_2 concentration.

4.4. *Transient flamelet analyses*

Transient flamelet profiles of the MILD and autoignitive flames from Fig. 4 are presented in Fig. 5. These results indicate that all flames begin to ignite at approximately 1.2 ms. This corresponds to initial ignition at 1.6, 1.8 and 2.0 x/D in the 3%, 6% and 9% O_2 coflows respectively, after this time is remapped to x/D using the stoichiometric flamelet

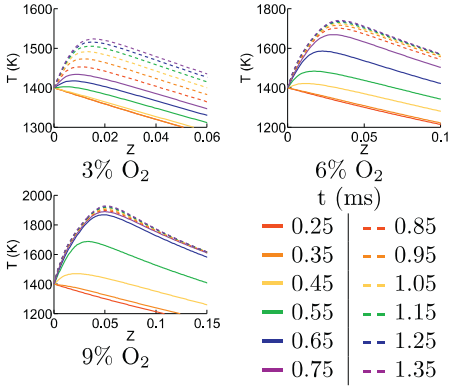

Fig. 6. T vs. Z profiles of transient flamelets at different times for C_2H_4 fuel in 1400-K coflows.

velocities for the respective values of Z_{st} [18]. The increasing heights with increasing O_2 are due to Z_{st} shifting towards regions of higher χ, delaying ignition. Following initial ignition, the flamelet in the 9% O_2 coflow reaches its maximum temperature by 2 ms, which is remapped to x/D of 2.6. This is shorter than the 6% O_2 case which takes 2.6 ms, corresponding to x/D of 2.7. The 3% O_2 case does not reach a steady temperature until approximately 5 ms, at x/D of 3.0, undergoing a significantly more gradual ignition process. These results replicate the experimentally observed trend, where the maximum chemiluminescence of flame in the 6% O_2 coflow appears higher than that in the 9% O_2 coflow and the flame in the 3% O_2 coflow initiates gradually, initially appearing closest to the jet exit plane. This is representative of the MILD combustion behaviour in the 3% O_2 case transitioning to autoignitive behaviour in the 9% O_2 case.

The effects of increased temperature on MILD flame stabilisation were assessed using transient flamelets with 1400-K oxidants. Fig. 3 indicates that all of these flames are within the MILD combustion regime. Temperature profiles from the transient analyses are shown in Fig. 6 with lines on each plot indicating increments of 0.10 ms from 0.25 ms to 1.35 ms. The profiles indicate ignition initiating after approximately 0.5 ms, 0.4 ms and 0.35 ms in the 3%, 6% and 9% O_2 oxidants, respectively. Flame temperatures reach steady-state values by 1.65 ms, 1.05 ms and 0.65 ms, at 1.9, 1.7 and 1.3 x/D, in the 3%, 6% and 9% O_2 oxidants, respectively. This shows that increases in coflow O_2 decrease the heights of both the initial ignition and the distance to reach a steady temperature and do not indicate any non-monotonic trend in lift-off height. In contrast, the flames in 1250-K coflows exhibit increasing heights before initial temperature increases with increasing O_2 concentration, demonstrating the effects of temperature, coupled with the imposed Z and χ fields. In the cooler 1250-K coflow, Z_{mr} shifts towards Z_{st} in regions of higher χ and lower velocity (described in the analysis of Fig. 5). Lower χ at Z_{mr} allows the flame in 3% O_2 coflow to stabilise closer to the jet exit plane than in the 6% O_2 case. With the increase to 9% O_2, the increased reactivity at Z_{mr} overcomes higher χ and the flame-base moves closer to the jet exit plane, as seen experimentally. This suggests that the non-monotonic trend in lift-off height seen experimentally indicates Z_{mr} shifts away from the coflow, into the high shear mixing layer, where autoignitive flames ignite more readily than MILD flames. This additionally explains the wider reaction zones under MILD conditions seen in previous work at lower temperatures [12], as the burning mixtures are confined by the low Z flammability limit and the high χ turbulent mixing layer.

5. Conclusions

A new non-premixed definition for MILD combustion, based on an equivalent activation energy rather than prior assessment of a reference temperature, was derived and shown to be consistent with previous experimental observations of gradual ignition. This definition incorporates, and consolidates, previous definitions of the MILD combustion conditions and the suggested combustion regimes which exhibit similar ignition behaviours. The new definition has shown good agreement with steady-state flamelet simulations, demonstrating better agreement than previous classifications between the simulated and predicted boundaries between the non-premixed MILD and autoignitive regimes. These boundaries show that non-premixed MILD combustion is achievable by minimising the overall temperature increase, or increasing initial temperatures and may be achieved following forced ignition.

Time-averaged chemiluminescent images of a series of flames showed that autoignitive flames exhibit peak temperatures at the flame-base, in contrast to the gradual ignition predicted and observed in MILD jet flames. Transient flamelet modelling indicated that the shift in ignition location from regions of low scalar dissipation rate towards the jet shear layer is responsible for the observed non-monotonic trend in flame lift-off heights. This shift towards shear layer is driven by decreasing temperature and increasing oxidant O_2 levels. This may also explain the decreasing reaction zone width in the transition to conventional autoignition. These results provide a better understanding of the boundaries and stabilisation of non-premixed flames in, and near, the MILD combustion regime.

Acknowledgements

The authors thank Ms Jingjing Ye for her assistance during experimental setup and flame imaging. The authors acknowledge support from

The University of Adelaide, Stanford University and the Politecnico di Milano. M.J.E. acknowledges financial support from the Endeavour Scholarships and Fellowship grant programme; P.R.M. and M.J.E. acknowledge financial support Australian Research Council (ARC) Discovery (DP and DECRA) grant scheme and the United States Asian Office for Aerospace Research and Development (AOARD); and H.W. and M.I. acknowledge financial support through NASA with award number NNX15AV04A.

References

[1] A. Cavaliere, M. de Joannon, Prog. Energy Combust. 30 (4) (2004) 329–366, doi:10.1016/j.pecs.2004.02.003.

[2] F.C. Christo, B.B. Dally, Combust. Flame 142 (1–2) (2005) 117–129, doi:10.1016/j.combustflame.2005.03.002.

[3] M. Ihme, Y.C. See, Proc. Combust. Inst. 33 (1) (2011) 1309–1317, doi:10.1016/j.proci.2010.05.019.

[4] P. Sabia, M. de Joannon, A. Picarelli, R. Ragucci, Combust. Flame 160 (1) (2013) 47–55, doi:10.1016/j.combustflame.2012.09.015.

[5] M. Oberlack, R. Arlitt, N. Peters, Combust. Theor. Model. 4 (4) (2000) 495–510, doi:10.1088/1364-7830/4/4/307.

[6] F. Wang, P. Li, Z. Mei, J. Zhang, J. Mi, Energy 72 (2014) 242–253, doi:10.1016/j.energy.2014.05.029.

[7] M.J. Evans, P.R. Medwell, Z.F. Tian, A. Frassoldati, A. Cuoci, A. Stagni, AIAA J. (2016). In Press, doi: 10.2514/1.J054958.

[8] F. Wang, J. Mi, P. Li, Energy Fuels 27 (6) (2013) 3488–3498, doi:10.1021/ef400500w.

[9] K. Bray, M. Champion, P.A. Libby, Combust. Flame 107 (1–2) (1996) 53–64, doi:10.1016/0010-2180(96)00014-4.

[10] M. Ihme, J. Zhang, G. He, B.B. Dally, Flow Turbul. Combust. 89 (2012) 449–464, doi:10.1007/s10494-012-9399-7.

[11] J.A. Sidey, E. Mastorakos, Combust. Flame 163 (2016) 1–11, doi:10.1016/j.combustflame.2015.07.034.

[12] P.R. Medwell, P.A.M. Kalt, B.B. Dally, Combust. Flame 152 (2008) 100–113, doi:10.1016/j.combustflame.2007.09.003.

[13] B. Choi, S. Chung, Combust. Flame 157 (12) (2010) 2348–2356, doi:10.1016/j.combustflame.2010.06.011.

[14] M.J. Evans, P.R. Medwell, Z.F. Tian, Combust. Sci. Technol. 187 (7) (2015) 1093–1109, doi:10.1080/00102202.2014.1002836.

[15] H. Pitsch, S. Fedotov, Combust. Theor. Model. 5 (1) (2001) 41–57, doi:10.1088/1364-7830/5/1/303.

[16] H. Pitsch, 1998. FlameMaster: A C++ computer program for 0D combustion and 1D laminar flame calculations. Available at URL: http://www.itv.rwth-aachen.de/downloads/flamemaster/.

[17] E. Ranzi, A. Frassoldati, R. Grana, et al., Prog. Energy Combust. Sci. 38 (4) (2012) 468–501, doi:10.1016/j.pecs.2012.03.004. Version: Dec. 2015. Current version of mechanism available from URL: http://creckmodeling.chem.polimi.it/

[18] H. Pitsch, M. Chen, N. Peters, Proc. Combust. Inst. 27 (1) (1998) 1057–1064, doi:10.1016/S0082-0784(98)80506-7.

[19] N. Peters, *Turbulent Combustion*, Cambridge Univer- sity Press, 2000.

[20] N. Peters, F.A. Williams, AIAA J. 21 (3) (1983) 423–429, doi:10.2514/3.8089.

[21] E. Mastorakos, Prog. Energy Combust. Sci. 35 (1) (2009) 57–97, doi:10.1016/j.pecs.2008.07.002.

[22] H. Wang, X. You, A. V. Joshi, et al. 2007. USC Mech Version II. High-Temperature Combustion Reaction Model of H2/CO/C1-C4 Compounds. Mechanism available from URL: http://ignis.usc.edu/USC_Mech_II.htm.

[23] N. Peters, F. Williams, Combust. Flame 68 (2) (1987) 185–207, doi:10.1016/0010-2180(87)90057-5.

[24] B. Dally, A. Karpetis, R. Barlow, Proc. Combust. Inst. 29 (1) (2002) 1147–1154, doi:10.1016/S1540-7489(02)80145-6.

[25] E. Oldenhof, M.J. Tummers, E.H. van Veen, D.J.E.M. Roekaerts, Combust. Flame 157 (6) (2010) 1167–1178, doi:10.1016/j.combustflame.2010.01.002.

[26] C.M. Arndt, R. Schießl, J.D. Gounder, W. Meier, M. Aigner, Proc. Combust. Inst. 34 (1) (2013) 1483–1490, doi:10.1016/j.proci.2012.05.082.

[27] R. Cabra, J.-Y. Chen, R. Dibble, A. Karpetis, R. Barlow, Combust. Flame 143 (4) (2005) 491–506, doi:10.1016/j.combustflame.2005.08.019.

[28] C.K. Westbrook, F.L. Dryer, Prog. Energy Combust. Sci. 10 (1) (1984) 1–57, doi:10.1016/0360-1285(84)90118-7.